Nanomed Res J 10(4):390-406, Autumn 2025

RESEARCH ARTICLE

Harnessing Exosomes for Natural Compound Delivery: Enhanced Antitumor Activity of Cinnamaldehyde in Colorectal Cancer Cells

Salwa Ahmed[1], Hanan. A. Soliman[1], Basant Mahmoud [1], Asmaa M. Mahmoud[1, *], Ahmed A. G. El-Shahawy[2]

[1] Department of Biochemistry, Faculty of Science, Beni-Suef University, Egypt.

[2] Materials Science and Nanotechnology Department, Faculty of Postgraduate Studies for Advanced Sciences (PSAS), Beni-Suef University, 62511 Beni-Suef, Egypt

ARTICLE INFO

Article History:
Received 21 Aug 2025
Accepted 16 Nov 2025
Published 01 Dec 2025

Keywords:
Colorectal cancer
Cinnamaldehyde
Exosome
Drug loading
Apoptosis

ABSTRACT

Cinnamaldehyde (CINAM), a natural compound with established anticancer properties, has limited clinical application due to its poor solubility and low bioavailability. Exosomes, which are cell-derived nanocarriers, offer a biocompatible platform for enhancing drug delivery and intracellular targeting. In this study, we evaluated the cytotoxic and molecular effects of CINAM-loaded mesenchymal stem cell–derived exosomes (EXO-CINAM) on colorectal cancer (Caco-2) cells. Exosomes were isolated and characterized using transmission electron microscopy (TEM), and CINAM loading was confirmed using high-performance liquid chromatography (HPLC). Cytotoxicity was assessed by sulforhodamine B (SRB) assay, apoptosis and cell cycle progression was analyzed by flow cytometry and DNA fragmentation assays, and ultrastructural changes were visualized by TEM. Western blotting and ELISA were employed to measure apoptotic protein expression, while qRT-PCR was used to examine gene expression related to apoptosis, inflammation, and angiogenesis. EXO-CINAM exhibited significantly greater cytotoxicity than free CINAM (IC_{50}: 23.87 µg/mL vs. 35.24 µg/mL, $p < 0.01$), with increased apoptosis (56.3% vs. 43.7%), G_0/G_1 apoptotic morphology confirmed by TEM, and DNA laddering indicating nuclear fragmentation. Protein analysis revealed elevated levels of cleaved caspase-3, -8, and -9, along with increased p53 and BAX levels and decreased BCL-2 levels. Gene expression analysis showed downregulation of NF-κB, MMP-2, MMP-9, and VEGFR2, and upregulation of CD95 and CD95L. IL-10 levels were also reduced, suggesting an anti-inflammatory effect of the treatment. Collectively, these findings indicate that exosomal delivery of CINAM enhances its anticancer activity by promoting apoptosis and suppressing inflammatory and angiogenic signaling, establishing EXO-CINAM as a promising nanotherapeutic platform for cancer treatment.

How to cite this article
Ahmed S., . A. Soliman H., Mahmoud B., M. Mahmoud A.,A. G. El-Shahawy A. Harnessing Exosomes for Natural Compound Delivery: Enhanced Antitumor Activity of Cinnamaldehyde in Colorectal Cancer Cells. Nanomed Res J, 2025; 10(4): 390-406.
DOI: 10.22034/nmrj.2025.04.007

INTRODUCTION

Colorectal cancer (CRC) is one of the most prevalent and lethal malignancies worldwide, particularly in industrialized nations [1]. It typically arises from the transformation of benign adenomatous polyps through a multistep process involving genetic and epigenetic alterations, ultimately resulting in invasive carcinoma and metastasis. CRC progression is influenced by a combination of hereditary factors, accounting for approximately 35% of cases, and modifiable risk factors, such as dietary habits, physical inactivity, obesity, smoking, and chronic inflammatory conditions of the colon [2]. Despite advances in screening techniques, including colonoscopy, fecal immunochemical tests, and stool DNA assays, late-stage diagnosis remains common, significantly reducing patient survival rates [3].

* Corresponding Author Email: *Ahmed.elshahawy@psas.bsu.edu.eg*

Current treatment options for CRC include surgical resection, chemotherapy, radiotherapy, targeted therapy, and immunotherapy [4]. Although these approaches have improved clinical outcomes, their efficacy is often limited by systemic toxicity, drug resistance, and poor tumor-specific targeting [5]. Consequently, there is a growing emphasis on developing novel therapeutic strategies that enhance efficacy while minimizing adverse effects. In this context, natural bioactive compounds and nanotechnology-based drug delivery systems have emerged as promising strategies for cancer treatment [6].

Cinnamaldehyde (CINAM), the principal active component of cinnamon bark extract, has garnered significant attention for its diverse pharmacological properties, including antioxidants, anti-inflammatory, antimicrobial, and anticancer properties [7]. Mechanistic studies have demonstrated that CINAM exerts cytotoxic effects on cancer cells by modulating key signaling pathways involved in apoptosis, oxidative stress, angiogenesis, and cell proliferation [8]. CINAM activates pro-apoptotic proteins, suppresses anti-apoptotic markers, reduces oxidative damage, and inhibits the growth and metastasis of various tumor types, including colorectal carcinoma [9].

Exosomes (EXOs) are nanosized extracellular vesicles (30–150 nm in diameter) secreted by most eukaryotic cells. They play a critical role in intercellular communication by transporting biologically active molecules, such as proteins, lipids, mRNAs, and microRNAs [10]. In cancer biology, exosomes are implicated in processes such as tumor progression, immune evasion and metastasis. Owing to their inherent stability, low immunogenicity, and ability to traverse biological barriers, exosomes are ideal candidates for drug delivery systems. Their capacity for tumor tropism and deep tissue penetration enhances the therapeutic potential of encapsulated agents while reducing off-target effects [11].

The integration of natural compounds, such as CINAM, into exosome-based delivery systems represents a novel strategy for enhancing anticancer efficacy through improved bioavailability, sustained release, and targeted action. However, few studies have evaluated the combined therapeutic effects of CINAM and exosome carriers, particularly in colorectal cancer. While previous studies have explored loading phytochemicals such as curcumin and resveratrol into exosomes, our study specifically utilizes exosomes derived from mesenchymal stem cells (MSCs). MSC-derived exosomes possess unique advantages including low immunogenicity, high biocompatibility, tumor-targeting ability, and abundant yield, making them particularly effective drug carriers for cancer therapy [12, 13].

The present investigation is considering among the first to systematically evaluate the anticancer efficacy and detailed molecular mechanisms of MSC-derived exosome-loaded cinnamaldehyde (EXO-CINAM) in human colorectal cancer cells (Caco-2). Prior reports primarily focus on other phytochemicals or cancer types, so this represents a novel application in CRC with a natural compound not extensively studied in this delivery context [14]. Regarding exosome-mediated delivery of small molecules and phytochemicals has been explored previously; however, our study differs from prior work in different keys, empirically supported ways e.g. While cinnamaldehyde-treated MSC exosomes have been reported in other disease contexts (for example, in a recent study evaluating BM-MSC exosomes treated with cinnamaldehyde for anti-inflammatory effects in chondrocytes), there is no prior report to our knowledge that evaluates MSC-derived exosome encapsulation of CINAM specifically for anti-CRC activity and mechanistic profiling in Caco-2 cells. Thus, our work extends cinnamaldehyde–EXO applications into the CRC field [15].

Moreover, many prior reports using MSC-exosomes in CRC focus on nucleic-acid cargo or single pathway readouts (for example, miRNA-mediated effects), or test exosomes in other disease models. In contrast, our manuscript presents a comprehensive battery of mechanistic endpoints in a CRC model, including quantitative cytotoxicity/ IC_{50}, Annexin V/PI apoptosis profiling, caspase activation (intrinsic and extrinsic), cell-cycle distribution, TEM ultrastructure, DNA fragmentation, ELISA protein quantification, and qRT-PCR of NF-κB/MMP/VEGFR2 pathways; allowing a systems-level interpretation of how EXO-CINAM exerts anti-tumor effects. This breadth of mechanistic data for a phytochemical loaded into MSC-exosomes in CRC has not been previously documented [16].

Finally, the present study aims to apply a sonication-assisted loading protocol and report loading efficiency, size distribution, and morphology of the drug-loaded vesicles. Although several reviews and studies document exosome loading strategies and examples with

curcumin/ resveratrol, explicit reporting of loading efficiency together with a functional, pathway-level readout in a CRC cell model is less common; our methodological transparency (parameters, dialysis/ultracentrifugation purification and HPLC quantitation) is intended to facilitate reproducibility and comparison with other cargo types [17].

Unlike many earlier studies addressing only cytotoxicity or uptake, the present investigation provides comprehensive mechanistic analysis via extensive characterizations of apoptotic pathways (intrinsic and extrinsic), cell cycle effects, inflammation, angiogenesis, and metastasis-related gene expression. This multi-dimensional mechanistic insight into how MSC-exosome delivery potentiates cinnamaldehyde's anticancer effects is uniquely detailed (Ababneh et al., 2025). Moreover, the present study applied a refined sonication-assisted loading method to maximize cinnamaldehyde encapsulation efficiency and preserve exosome integrity, with thorough physicochemical characterization. This optimization contributes to reproducibility and translational potential beyond previous crude formulations reported [12].

The combination of (i) MSC-sourced exosomes, (ii) cinnamaldehyde cargo applied to colorectal cancer cells, (iii) explicit encapsulation optimization and quantitative reporting, and (iv) an integrated, multi-assay mechanistic characterization that elucidates how EXO-CINAM modulates apoptotic, inflammatory, and angiogenic pathways is what makes our study novel, rather than the general idea of exosome-mediated phytochemical delivery per se.

Therefore, this study aimed to investigate the synergistic anticancer effects of exosome-loaded cinnamaldehyde (EXO-CINAM) in a human colorectal cancer cell model (Caco-2). Specifically, we evaluated the impact of this combination on multiple cellular processes, including proliferation, apoptosis (via intrinsic and extrinsic pathways), cell cycle progression, angiogenesis, and inflammatory signaling. This study aimed to establish a mechanistic foundation for the development of exosome-mediated delivery of natural compounds as a promising therapeutic approach for CRC treatment.

MATERIALS AND METHODS

Chemicals and Reagents

Cinnamaldehyde (CINAM; purity ≥99%; CAS No. 14371-10-9) was purchased from Carlo Erba (Milan, Italy). Ethanol (analytical grade), phosphate-buffered saline (PBS), and all other chemicals were obtained from Sigma-Aldrich (St. Louis, MO, USA), unless otherwise stated. Fetal bovine serum (FBS), RPMI-1640 medium, penicillin–streptomycin, and trypsin–EDTA were procured from Gibco (Thermo Fisher Scientific, USA). All reagents were prepared using sterile techniques.

Cell Line and Culture Conditions

The human colorectal adenocarcinoma cell line Caco-2 was obtained from Nawah Scientific, Inc. (Cairo, Egypt) and cells were cultured in RPMI-1640 medium supplemented with 10% heat-inactivated FBS and 1% penicillin–streptomycin and maintained in a humidified incubator at 37 °C with 5% CO_2. Cells were subculture at 80–90% confluence using 0.25% trypsin–EDTA. The RPMI-1640 formulation was employed in this study following the conditions provided and validated by Nawah Scientific Inc. (Cairo, Egypt), a certified supplier of the Caco-2 cell line. Their culture conditions are based on some previous studies, which have also successfully maintained Caco-2 cells in RPMI medium with comparable phenotypic and metabolic characteristics to those cultured in DMEM [18, 19].

Preparation of Cinnamaldehyde Stock Solution

A 1 mg/mL stock solution of CINAM was prepared in absolute ethanol and stored at 4 °C, protected from light. Working dilutions were freshly prepared in a 1:1 ethanol–water mixture for experimental use.

Exosome Isolation from Mesenchymal Stem Cells

All experiments were conducted in compliance with institutional guidelines for research involving biological materials. Rat bone marrow mesenchymal stem cells (rBM-MSCs) were commercially sourced from a Nawah Scientific Inc. (Cairo, Egypt), the certified supplier of the Caco-2 cell line used in our experiments, and therefore, no animal experiments were performed directly by the authors. Therefore, the institutional approval for animal use was not required for this study. The culture supernatants were subjected to differential centrifugation at 300 ×g for 10 min, 1,000 ×g for 20 min, and 10,000 ×g for 30 min to remove debris and apoptotic bodies. The supernatant was then filtered through 0.22 μm syringe filters and

ultracentrifuged at 100,000 ×g for 90 min at 4 °C. The resulting exosomal pellet was resuspended in PBS and quantified using a bicinchoninic acid (BCA) protein assay kit (Novagen, Darmstadt, Germany) following the manufacturer's protocol [20]. In addition, owing to resource limitations, the present study did not perform surface marker profiling (e.g., CD9, CD63, and CD81) in this investigation, even though TEM confirmed the characteristic spherical bilayer-bound vesicles of ~30-150 nm. Such profiling is advised for complete EV/exosome " validation in accordance with the ISEV MISEV2018 criteria [21].

Preparation of Exosome-Loaded Cinnamaldehyde (EXO-CINAM)

CINAM was encapsulated into exosomes using a sonication-assisted loading method adapted from Haney et al. (2015). Briefly, exosomes (200 µg/mL protein concentration) were mixed with CINAM at a 1:10 drug-to-exosome ratio (w/w) and sonicated using a probe sonicator (10 cycles of 30s on/30 s off at 20% amplitude). The mixture was incubated at 37 °C for 1 h and dialyzed against PBS using a 3.5 kDa MWCO dialysis membrane to remove the unbound drug. The final formulation (EXO-CINAM) was filtered through a 0.22 µm membrane and stored at 4 °C until use [22].

Characterization of Exosomes and EXO-CINAM
Transmission Electron Microscopy (TEM)

The morphology and size of the exosomes were evaluated using transmission electron microscopy (TEM; JEOL JEM-1400, Japan) [23]. They detail the examination of exosome morphology using the JEOL JEM-1400 TEM and offer procedural specifics for fixation, staining, and imaging. Briefly, the samples were fixed in 2% paraformaldehyde, loaded onto formvar-coated grids, and negatively stained with 1% uranyl acetate. After drying, the grids were imaged at 80 kV. The diameters of roughly 50–75 individual vesicles were measured using ImageJ software to ascertain the average size and distribution of the 8–10 TEM images that were prepared for this study. These images were taken at random. In addition, two qualified authors carried out the current counting and measurements separately to guarantee precision and repeatability.

High-Performance Liquid Chromatography (HPLC)

Moreover, to clarify, after exosome loading, the formulation underwent two sequential purification steps to ensure the complete removal of unbound (free) cinnamaldehyde (CINAM). First, the suspension was subjected to dialysis using a 12–14 kDa molecular weight cut-off (MWCO) membrane against phosphate-buffered saline (PBS) at 4 °C for 24 h, with buffer changes every 4 h. Second, following dialysis, the sample was ultracentrifuged at 100,000 × g for 70 minutes at 4 °C, and the supernatant was discarded. HPLC analysis of the supernatant revealed no detectable free CINAM, confirming removal. This combined method is consistent with current best practices in the EV field for separating drug-loaded vesicles from free drug molecules, as outlined in recent reviews on drug-loaded extracellular vesicle purification [24-26]. The loading efficiency of CINAM into exosomes was quantified using high-performance liquid chromatography (HPLC; Waters 2690 Alliance system, USA) equipped with a photodiode array detector set at 290 nm. Separation was achieved using a C18 Inertsil ODS column (4.6 × 250 mm, 5 µm) with an isocratic mobile phase of 0.1% phosphoric acid: acetonitrile (80:20, v/v) at a flow rate of 1.0 mL/min. The injection volume was 20 µL. A calibration curve of CINAM (10–80 µg/mL) was used for quantification of CINAM.

Experimental Design and Treatment Groups

Caco-2 cells were seeded in 6-well plates at a density of 5×10^4 cells/well and incubated for 24 h before treatment. The cells were divided into four groups: Control group (C): Untreated Caco-2 cells, CINAM group: Caco-2 cells treated with CINAM (20 µg/mL), EXO group: Caco-2 cells treated with exosomes (20 µg/mL protein) and EXO-CINAM group: Caco-2 cells treated with CINAM-loaded exosomes (equivalent to 20 µg/mL CINAM). All treatments were applied for 48 h, unless otherwise stated.

Cytotoxicity Assay

Cell viability was assessed using the sulforhodamine B (SRB) assay. After 72 h of treatment, the cells were fixed in cold 10% trichloroacetic acid, stained with 0.4% SRB solution, washed with 1% acetic acid, and solubilized in 10 mM Tri's base. Absorbance was measured at 540 nm using a microplate reader (BioTek, USA). Inhibitory Concentration 50% (IC_{50}) values were calculated from dose–response curves. Since the SRB assay measures total protein content and total cell mass following prolonged treatment, a 72-hour

exposure time was selected to capture cumulative harmful effects and precisely calculate the IC_{50}. This duration considers the slow action of natural substances and exosome-based systems and is consistent with the standard procedure in Caco-2 cell drug screening. As demonstrated by lower cell viability at 72 h than at shorter exposures, longer incubation guarantees consistent dose–response relationships and more accurate viability assessments. To precisely determine the cytotoxicity and IC_{50} in Caco-2 cells, particularly for drugs with delayed effects, our final selection for the 72-hour exposure is ideal [27].

Flow Cytometry Analysis

Cell Cycle Distribution

Cells were harvested, fixed in 70% ethanol, and stained with propidium iodide (PI, 50 µg/mL) containing RNase A (100 µg/mL) for 30 min at 37 °C. Samples were analyzed using a CytoFLEX flow cytometer (Beckman Coulter, USA), and the cell cycle phases were quantified using CytExpert 2.3 software.

Apoptosis Detection

Apoptosis was evaluated using Annexin V–FITC/PI dual staining (Miltenyi Biotech, Cat #130-092-052). After 48 h of treatment, the cells were stained for 15 min at room temperature in the dark, and fluorescence was recorded using a CytoFLEX flow cytometer. A 48-hour incubation was chosen to capture apoptosis and cell cycle changes occurring early after drug exposure, while avoiding excessive loss of cells or secondary necrosis. This timeframe effectively detects apoptotic events, cell cycle arrest, and phosphatidylserine externalization, aligning with published Caco-2 data showing significant changes within 24–48 hours [28].

Transmission Electron Microscopy of Treated Cells

Treated and untreated Caco-2 cells (24- and 48-hours post-treatment) were fixed in 2.5% glutaraldehyde, post-fixed in osmium tetroxide, dehydrated through a graded ethanol series, embedded in epoxy resin, sectioned (70 nm), and stained with uranyl acetate and lead citrate. The samples were examined using a JEOL JEM-1400 TEM.

DNA Fragmentation Assay

Genomic DNA was extracted following the instruction of the Quick-gDNA™ MiniPrep kit (Zymo Research, USA). DNA fragmentation was assessed using 1.5% agarose gel electrophoresis. The DNA concentration was determined spectrophotometrically at 260 nm.

Western Blotting

Total protein was extracted using the ReadyPrep™ Protein Extraction Kit (Bio-Rad, USA). Briefly, proteins (30 µg/lane) were separated using SDS-PAGE and transferred onto PVDF membranes. Membranes were blocked with 5% non-fat milk and incubated overnight at 4 °C with primary antibodies against caspase-3, caspase-8, caspase-9, and β-actin (loading control). HRP-conjugated secondary antibodies were applied, and bands were visualized using chemiluminescent substrate and imaged with a ChemiDoc™ MP system (Bio-Rad).

ELISA Assays

Quantitative ELISA kits were used to detect the protein levels of p53 (BMS256), BAX (EEL030), BCL-2 (BMS244-3), cytochrome c (BMS263), and IL-10 (BMS215-2), according to the manufacturers' instructions (Thermo Fisher Scientific). The absorbance was measured at 450 nm.

Quantitative Real-Time PCR (qRT-PCR)

Total RNA was isolated using the Qiagen RNeasy Mini Kit, and cDNA was synthesized using the High-Capacity cDNA Reverse Transcription Kit (Applied Biosystems). qRT-PCR was performed using SYBR Green Master Mix on a Step OnePlus™ Real-Time PCR system. The primers targeted NF-κB, MMPs, CD95, CD95L, and VEGFR2. Relative expression was calculated using the $2^{-\Delta\Delta Ct}$ method, with GAPDH as the internal control. The present work aims to evaluate mechanistic alterations (caspases, Bcl-2 family, NF-κB/MMP/VEGFR2) during the stage of the greatest signaling response, these endpoints were timed to coincide with the 48-hour flow cytometry point. Coherent interpretation is ensured, and variability is decreased by this assay alignment. Additionally, to ensure uniformity across mechanistic readouts and to align with the time of peak apoptotic signaling seen in flow cytometry, these studies were timed to coincide with the 48-hour treatment point [29].

Statistical Analysis

Data is presented as the mean ± standard deviation (SD) from at least three independent

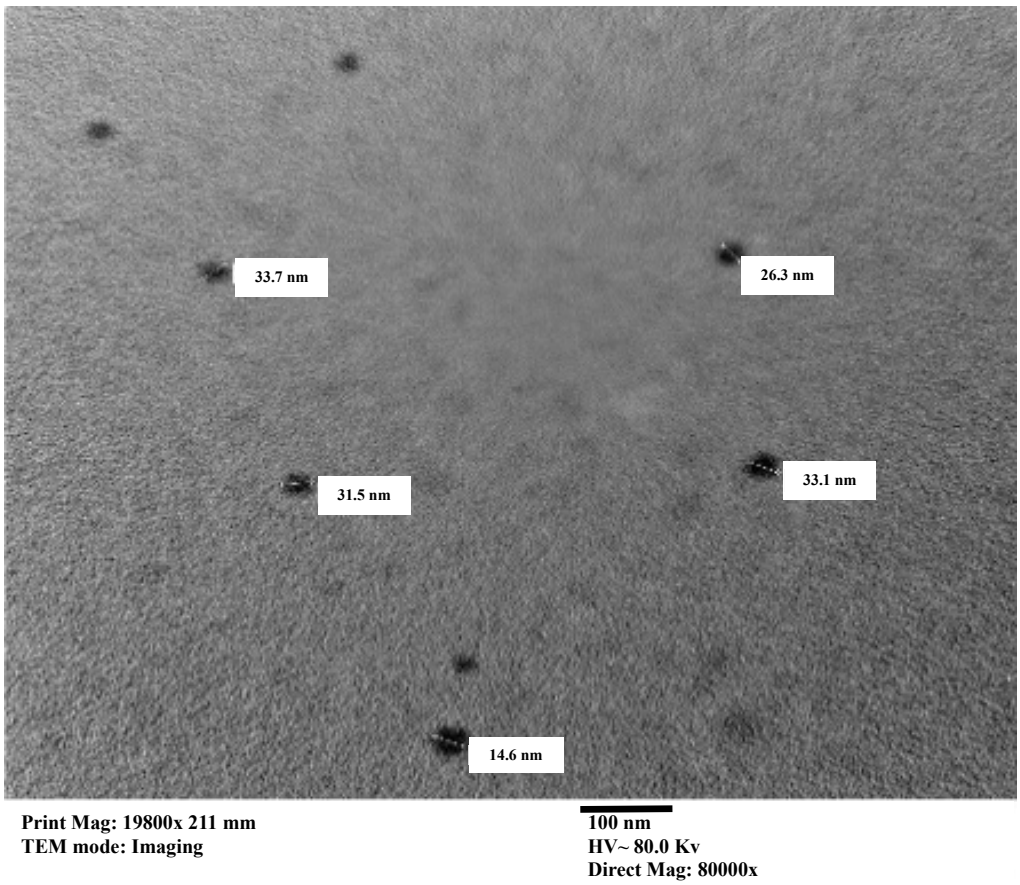

Fig. 1. Transmission electron micrographs (JEOL (JEM-1400 TEM) of mesenchymal stem cell–derived exosomes. Representative TEM images show rounded, bilayer-bounded vesicles within the expected exosome size range (30–150 nm). Scale bars = 100 nm.

experiments. Statistical analysis was performed using IBM SPSS Statistics v26.0 (IBM Corp., Armonk, NY). Means for groups in homogeneous subsets are displayed the subset of alpha = 0.05. and all values were represented as Mean ± Std & n = 3 replicates (three independent biological replicates) and repeated twice for each cell group. Means that within the same conditions and not sharing a common superscript symbol(s), differ significantly at *$p < 0.05$, $p < 0.01$ vs. control. Superscripts represent significant post-Hoc one-way ANOVA results of improvement over time. Data was analyzed using Duncan's method for post-hoc analysis to compare various groups with each other.

RESULTS

Characterization of Exosomes and Cinnamaldehyde Loading

Figure 1 shows a TEM image of exosomes isolated from the mesenchymal stem cell–derived conditioned medium. The exosomes appeared as well-defined, spherical vesicles with diameters ranging from approximately 14.6 nm to 33.7 nm. These nanoscale dimensions fall within the expected size range for exosomes (30–150 nm), confirming successful isolation. The vesicles exhibited a uniform morphology and discrete membrane boundaries, indicating structural integrity. This image supports the morphological criteria for exosomal identity, consistent with previously published reports. No significant morphological alterations were observed following CINAM loading into the exosomes, confirming structural preservation.

The calibration curve for CINAM based on HPLC analysis, plotting the peak area against standard concentrations ranging from 10 to 80 µg/mL (Figure 2). The calibration data demonstrated excellent linearity across this concentration range, with a regression equation of y = 109,492.324x

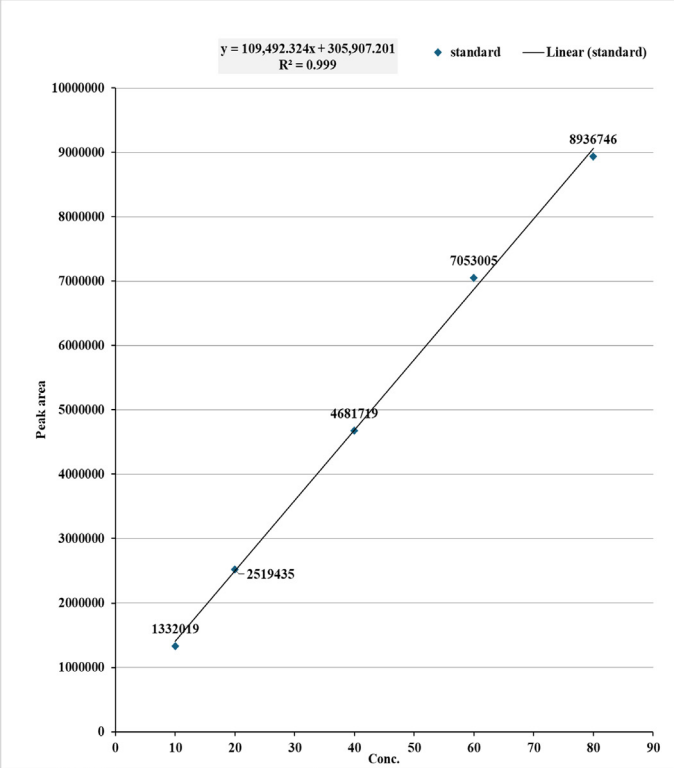

Fig. 2. Calibration curve and chromatogram of cinnamaldehyde (CINAM) by HPLC. The inset displays the standard calibration curve (10–80 µg/mL) with excellent linearity (R^2 = 0.999). The chromatogram shows the CINAM retention peak at 7.2 min used to determine loading efficiency.

+ 305,907.201 and a correlation coefficient (R^2 = 0.999), indicating a strong linear relationship between the concentration and peak response. This high degree of linearity ensured the accuracy and reliability of the quantitative determination of CINAM in the experimental samples. Thus, the method was validated for the precise calculation of loading efficiency and drug content in exosome-based formulations. Drug-loading efficiency was evaluated using HPLC. The CINAM peak was identified at a retention time of 7.2 min. Quantitative analysis confirmed a loading efficiency of 38.7 ± 1.2%, with consistent recovery across replicates.

Cytotoxicity and IC_{50} Determination

The cytotoxic effects of CINAM, exosomes (EXO), and CINAM-loaded exosomes (EXO-CINAM) on Caco-2 cells were assessed using a sulforhodamine B (SRB) assay. CINAM reduced cell viability in a concentration-dependent manner, with an IC_{50} value of 35.24 ± 1.8 µg/mL. EXO-CINAM demonstrated a significantly enhanced inhibitory effect, with an IC_{50} of 23.87 ± 1.3 µg/mL (mean ± SD, n = 3; one-way ANOVA, F = 41.22, p < 0.001; Tukey's post hoc test, p < 0.01 vs. CINAM group). Exosomes alone did not significantly affect the cell viability (Figure 3).

Apoptosis Induction by Annexin V–FITC/PI Staining

To evaluate apoptosis, flow cytometry was performed after Annexin V–FITC/PI dual staining. EXO-CINAM significantly increased the proportion of total apoptotic cells (early + late apoptosis: 56.3 ± 3.4%) compared to CINAM alone (43.7 ± 2.9%), EXO (9.8 ± 1.7%), and untreated controls (7.6 ± 2.1%) (n = 3 per group; F = 76.55, p < 0.001; Figure 4). No significant differences were observed between the EXO and control groups (p > 0.05).

Cell Cycle Distribution Analysis

Cell cycle progression was analyzed using propidium iodide (PI) staining and flow cytometry. Both CINAM and EXO-CINAM treatment induced G_0/G_1 phase arrest in Caco-2 cells. EXO-CINAM resulted in 61.4 ± 2.2% of cells in the G_0/G_1 phase,

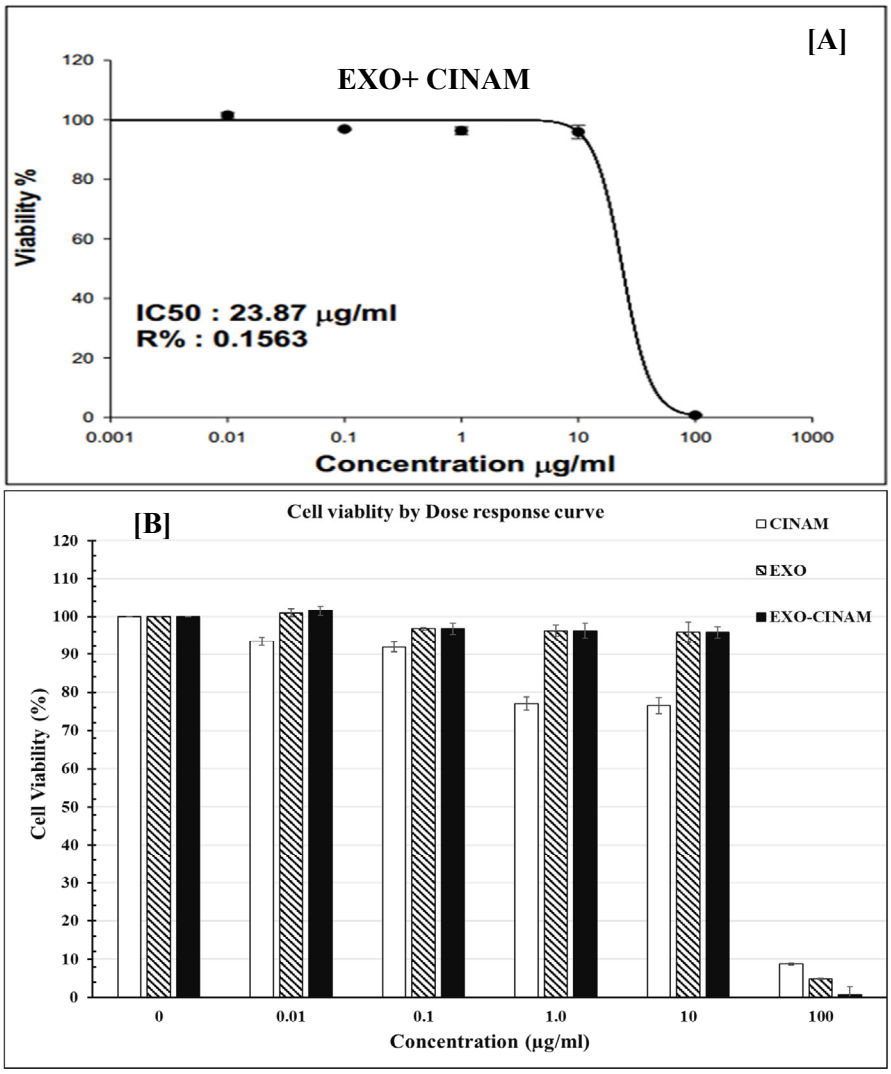

Fig. 3. Cell viability by dose–response curve Cell Viability (%) Treatments:(A) Dose–response curves obtained by SRB assay after 72 h treatment. (B) Bar graph comparing mean cell viability (%) of each group relative to control. Data represents Means± SD (n = 3), whereas CINAM (white bar graph), EXO (striped bar graph) and EXO–CINAM (black bar graph) and IC_{50} determination of free CINAM, EXO, and EXO-CINAM in Caco-2 cells.

significantly higher than that in the CINAM (49.6 ± 1.9%), EXO (37.5 ± 2.4%), and control (36.2 ± 2.5%) groups ($n = 3$; one-way ANOVA, $F = 46.9$, $p < 0.001$; Figure 5). The reductions in the S and G_2/M populations were proportional and statistically significant.

Ultrastructural Evaluation by TEM

Ultrastructural features were assessed 48 h post-treatment using TEM. CINAM- and EXO-CINAM–treated cells exhibited condensed chromatin, nuclear fragmentation, cytoplasmic vacuolization, and apoptotic bodies (Figure 6B, 6C). Mitochondrial swelling and disrupted membrane integrity were more pronounced in EXO-CINAM–treated cells. In contrast, cells treated with EXO or left untreated retained normal ultrastructure with intact nuclear and cytoplasmic features (Figure 6A, 6D).

DNA Fragmentation Assay

Apoptosis-associated DNA fragmentation was confirmed using agarose gel electrophoresis. DNA fragmentation analysis revealed characteristic apoptotic DNA laddering patterns in treated Caco-2 cells (Figure 7 and Table 1). Lane M, the

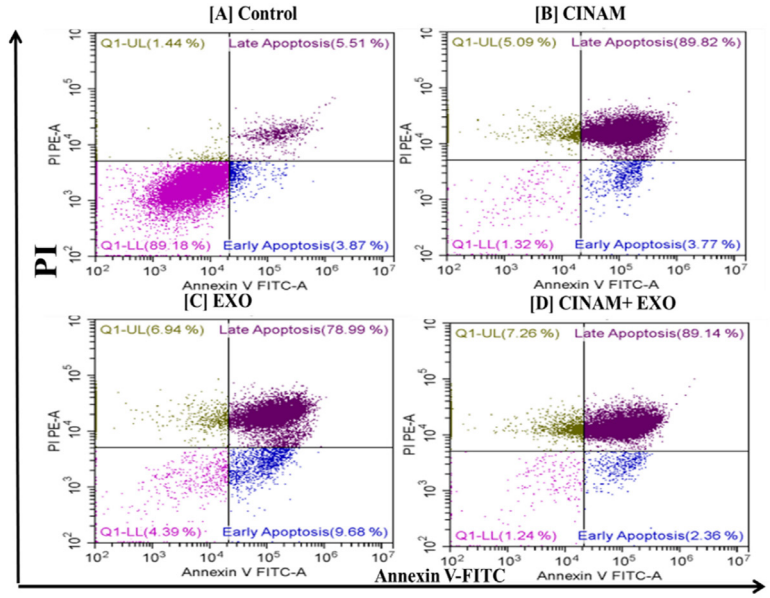

Fig. 4. Apoptosis analysis of Caco-2 cells by Annexin V–FITC/PI staining (using Propidium iodide; PI) after 48h treatment. Flow-cytometric dot plots showing early and late apoptotic populations. whereas panel [A] controls Caco-2 cells without any treatments; panel [B] treatment with CINAM; panel [C] treatment with EXO and panel [D] treatment with CINAM+ EXO. Quantitative data demonstrate a significant increase in apoptosis in the EXO-CINAM group compared with CINAM and control. Mean ± SD (n = 3)

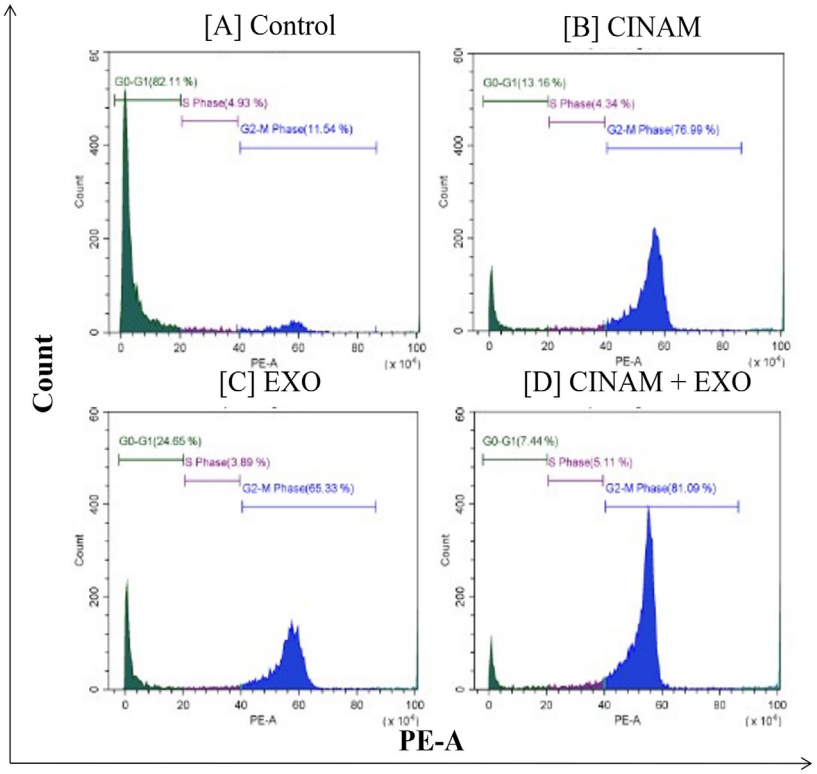

Fig. 5. Cell-cycle distribution of Caco-2 cells treated with CINAM or EXO-CINAM (48 h). Histograms from propidium iodide (PI)/RNase staining using flow cytometry indicate G_0/G_1 phase arrest following treatment. whereas panel [A] controls Caco-2 cells without any treatments; panel [B] treatment with CINAM; panel [C] treatment with EXO and panel [D] treatment with CINAM+ EXO. Percentages of cells in each phase were quantified using CytExpert 2.3 software.

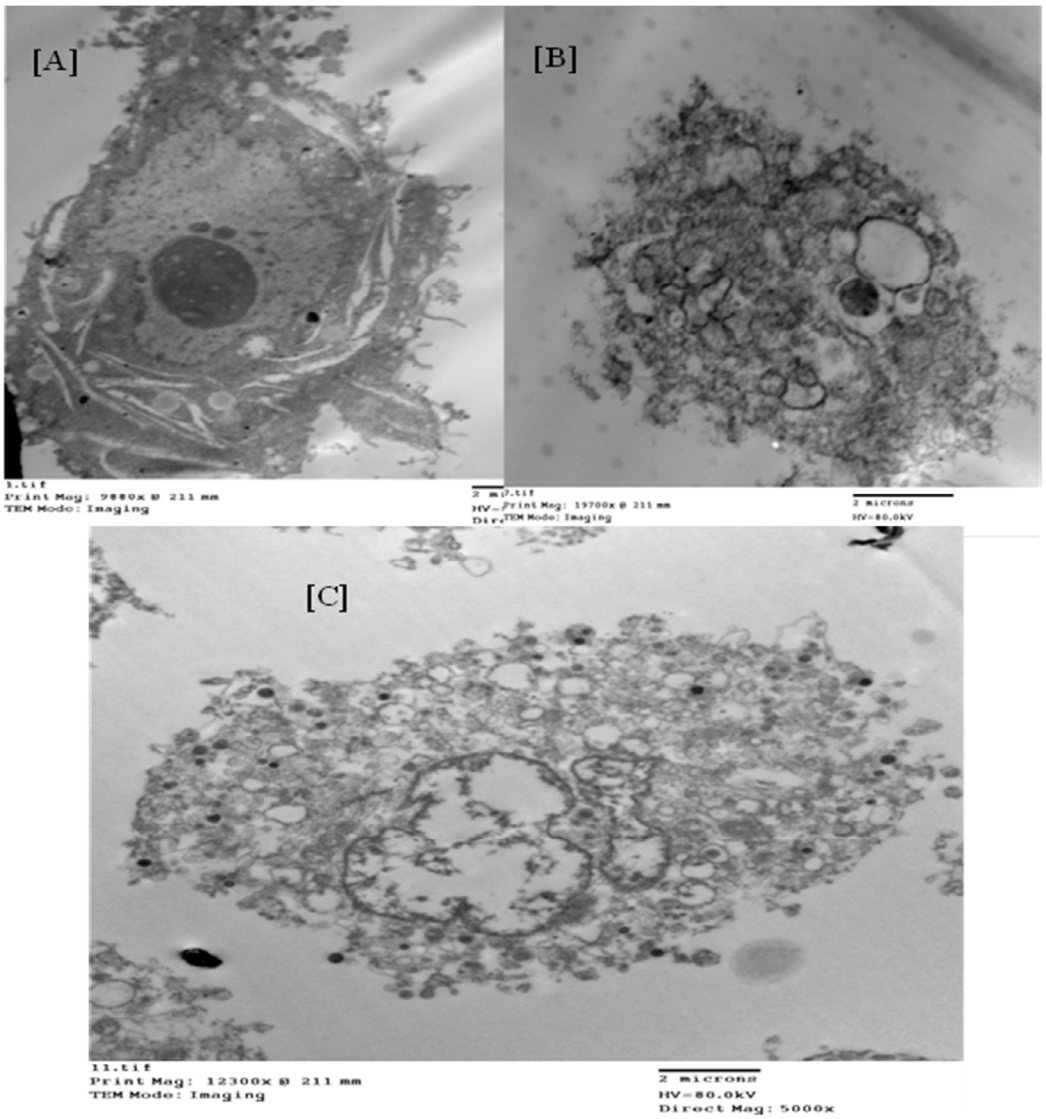

Fig. 6. Ultrastructural images examined by transmission electron microscope JEOL (JEM-1400 TEM) of treated Caco-2 cells. [A] Image of control cell of Colorectal Cancer cell line (Caco-2), [B] Image of Colorectal Cancer cell line (Caco-2) 24h after treated with CINAM+EXO, [C] Image of Colorectal Cancer cell line (Caco-2) 48h after treated with CINAM+EXO. Control and EXO groups show intact nuclei and cytoplasmic morphology, while CINAM and EXO-CINAM groups exhibit chromatin condensation, mitochondrial swelling, and apoptotic bodies.

DNA Marker (100 bp ladder), shows distinct bands at expected intervals (100, 200, 300, 400, 500 bp, etc.), serving as a molecular reference. Lanes 2 and 3 for untreated Caco-2 cells show a single intact, high–molecular-weight DNA band near the top of the gel, with no laddering pattern, indicating that genomic DNA remains intact, which is typical of viable/non-apoptotic cells i.e. high-molecular-weight DNA bands with no apparent fragmentation, indicating preserved genomic integrity. Moreover, lanes 4 and 5 for the CINAM-treated cells show a clear DNA fragmentation ladder, showing multiple bands at ~200, 400, 600, 800, and 1,000 bp. This pattern reflects oligonucleosomal DNA fragmentation, a hallmark of apoptosis, confirming that CINAM induces apoptotic cell death. Lanes 6 and 7 show EXO–CINAM co-treatment showing a stronger and more defined laddering pattern than CINAM alone, revealing bands at approximately 200, 400, 600, 800, 1,000, and 1,200 bp, suggesting enhanced apoptotic DNA fragmentation, supporting a synergistic apoptotic effect of EXO–CINAM. Finally, lanes 8 and 9 (EXO-treated cells)

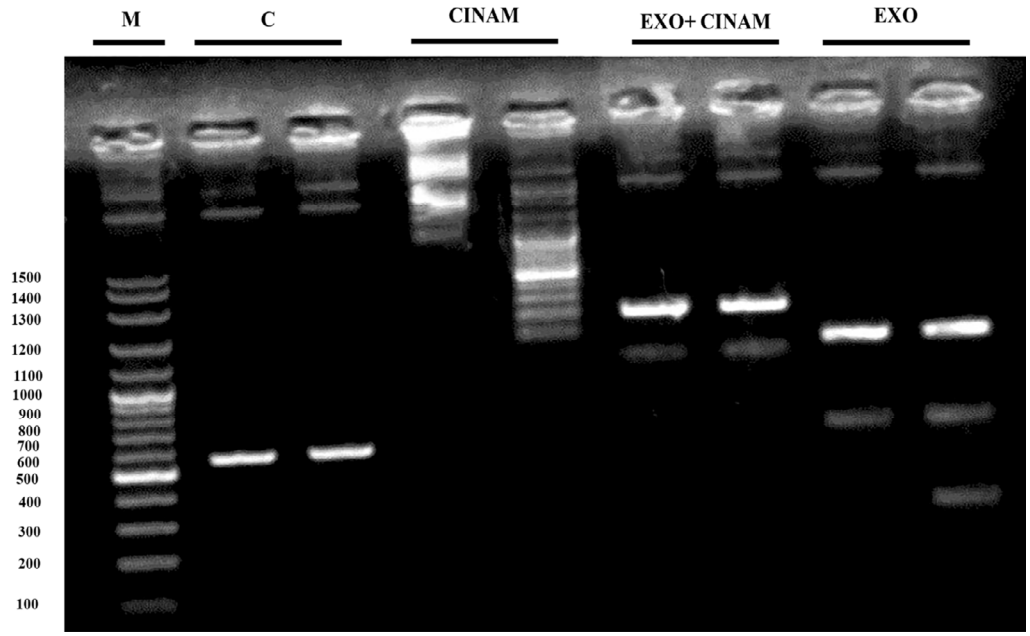

Fig. 7. DNA fragmentation assay of Caco-2 cells following treatment. Agarose gel electrophoresis (1.5%) showing characteristic DNA laddering (~200 bp multiples) in CINAM and EXO-CINAM groups, consistent with apoptosis induction. Lane M = 100 bp DNA marker; Lanes 2–3 = Control; Lanes 4–5 = CINAM; Lanes 6–7 = EXO-CINAM; Lanes 8–9 = EXO.

Table 1. DNA fragmentation values (optical density units, O.D / 260) in Caco-2 cells after 48 h treatment. Higher fragmentation indicates greater apoptotic activity

Groups	Control	CINAM	EXO	CINAM +EXO	F value	P <
DNA Fragmentation	2.01± 0.09^{d}	1.51± 0.08^{c}	1.02± 0.08^{b}	0.63± 0.06^{a}	360.11	0.000

Means for groups in homogeneous subsets are displayed the subset of alpha = 0.05. and all values were represented as Mean ± Std & n = 3 replicates and repeated twice for each cell group. Means that within the same conditions and not sharing a common superscript symbol(s), differ significantly at *p < 0.05, p < 0.01 vs. control. Superscripts represent significant post-Hoc one-way ANOVA results of improvement over time. Data was analyzed using Duncan's method for post-hoc analysis to compare various groups with each other.

showed that DNA remained largely intact with no clear laddering; faint smearing may be present, indicating minimal or no apoptosis, suggesting that EXO alone are less cytotoxic under these conditions.

Protein Expression Analysis

Western Blotting

The protein expression levels of cleaved caspase-3, -8, and -9 were evaluated. CINAM and EXO-CINAM treatments significantly upregulated all three caspases compared to the control and EXO-only groups. Quantitative densitometry indicated that EXO-CINAM induced higher expression of cleaved caspase-3 (2.8-fold), caspase-8 (2.1-fold), and caspase-9 (3.0-fold) compared to CINAM (n = 3; F = 19.32–28.46; $p < 0.001$; Figure 8A).

ELISA Quantification

ELISA assays revealed that EXO-CINAM treatment significantly increased the expression of pro-apoptotic proteins p53 (42.1 ± 2.5 pg/mL) and BAX (55.3 ± 3.1 pg/mL) and decreased the expression of anti-apoptotic BCL-2 (18.4 ± 1.6 pg/mL) compared to CINAM, EXO, and control (n = 3; all $p < 0.001$; Figure 8B). Cytochrome c levels were significantly elevated. Notably, IL-10 levels were reduced in the CINAM (21.6 ± 2.2 pg/mL) and EXO-CINAM (14.8 ± 1.9 pg/mL) groups compared to the control group (33.4 ± 2.6 pg/mL) ($p < 0.01$), suggesting anti-inflammatory activity. The results are presented in Table 2.

Gene Expression by qRT-PCR

Relative gene expression was analyzed using

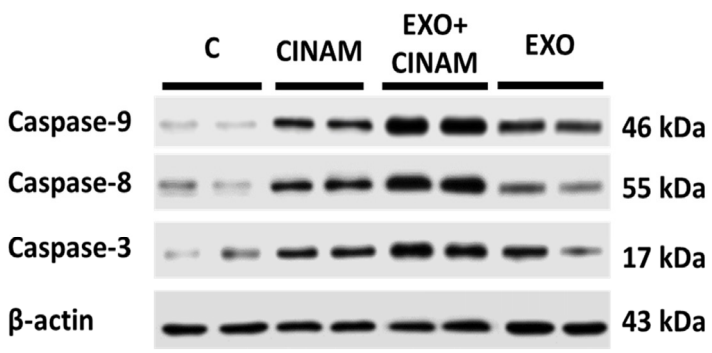

Fig. 8. Estimation of the protein expression of apoptotic markers using Western blot analysis of cleaved caspase-3, -8, and -9 in treated Caco-2 cells. Whereas Lanes 1–2 for Controls (C); Lanes 3–4 for CINAM-treated group; Lanes 5–6 for EXO-CINAM-treated group; Lanes 7–8 for EXO-treated group.

Table 2. ELISA quantification of apoptotic and inflammatory proteins (p53, BAX, BCL-2, cytochrome c, and IL-10 levels) in Caco-2 cells (48 h).

Groups	P53	BAX	Bcl2	CYC	IL-10
Control	1.11± 0.11^{a}	0.98± 0.17^{a}	3.07± 0.14^{d}	99.65± 12.14^{a}	173.03±6.31^{d}
CINAM	1.94± 0.25^{b}	2.12± 0.05^{b}	2.20± 0.01^{c}	157.72±11.57^{b}	95.95± 7.17^{c}
EXO	1.99± 0.13^{b}	2.07± 0.07^{b}	1.99± 0.11^{b}	152.20±10.75^{b}	78.65± 2.98^{b}
CINAM +EXO	2.68± 0.13^{c}	2.80± 0.11^{c}	1.02± 0.11^{a}	200.68±11.86^{c}	50.97± 1.73^{a}
F value	90.31	287.95	388.53	76.57	637.05
P <	0.0001	0.0000	0.0001	0.0001	0.0000

Means for groups in homogeneous subsets are displayed the subset of alpha = 0.05. and all values were represented as Mean ± Std & n = 3 replicates and repeated twice for each cell group. Means that within the same conditions and not sharing a common superscript symbol(s), differ significantly at *p < 0.05, p < 0.01 vs. control. Superscripts represent significant post-Hoc one-way ANOVA results of improvement over time. Data was analyzed using Duncan's method for post-hoc analysis to compare various groups with each other.

the 2–ΔΔCt method. EXO-CINAM significantly downregulated NF-κB, MMP-2, MMP-9, and VEGFR2 compared to the other groups ($p < 0.001$; $n = 3$; Figure 9). Conversely, CD95 and CD95L were markedly upregulated in the EXO-CINAM group (4.3-fold and 3.7-fold increases, respectively, compared to the control). These changes indicate concurrent modulation of intrinsic, extrinsic, and angiogenesis-related pathways, along with the suppression of inflammatory and angiogenic signaling. The results are presented in Table 3. Across multiple assays, EXO-CINAM consistently demonstrated greater efficacy than free CINAM in promoting apoptosis, inhibiting cell proliferation, and modulating the key signaling pathways. The exosome-based delivery system improved CINAM bioactivity, as evidenced by enhanced cytotoxicity, greater caspase activation, stronger gene regulation, and increased apoptotic markers without inducing off-target toxicity, highlighting EXO-CINAM as a superior formulation with increased bioactivity and targeted cellular uptake.

DISCUSSION

This study demonstrated that exosome-mediated delivery of CINAM enhances its anticancer efficacy in CRC cells. The formulation significantly improved CINAM's cytotoxicity, apoptotic activity, and suppression of proinflammatory and proangiogenic mediators. These findings align with and extend the existing evidence supporting the use of exosomes as efficient biocompatible nanocarriers for small molecules and phytochemicals.

Our results are consistent with those of previous studies reporting that CINAM induces apoptosis through both mitochondrial and death receptor pathways in various cancer models, including colorectal, gastric, and breast cancers [30]. Consistent with these reports, we observed upregulation of cleaved caspase-3, -8, and -9, along with increased p53 and BAX expression and downregulation of BCL-2 in Caco-2 cells.

Table 3. Relative mRNA expression of selected genes determined by qRT-PCR. Fold change relative to control calculated using the $2^{-\Delta\Delta Ct}$ method. Down-regulated genes are shaded in gray

Groups	NFkB	MMPs	CD95	CD95L	VEGFR2
C	1.17± 0.04[d]	1.07± 0.05[d]	1.01± 0.01[a]	1.01± 0.01[a]	1.11± 0.09[d]
CINAM	0.78± 0.03[c]	0.72± 0.05[c]	2.32± 0.08[b]	2.47± 0.12[b]	0.71± 0.02[c]
EXO	0.57± 0.06[b]	0.52± 0.04[b]	2.55± 0.05[c]	3.01± 0.14[c]	0.48± 0.03[b]
CINAM +EXO	0.29± 0.03[a]	0.13± 0.01[a]	3.83± 0.08[d]	3.62± 0.07[d]	0.20± 0.01[a]
F value	543.18	584.34	2262.97	777.90	396.94
P <	0.0001	0.000	0.0001	0.0001	0.0001

Means for groups in homogeneous subsets are displayed the subset of alpha = 0.05. and all values were represented as Mean ± Std & n = 3 replicates and repeated twice for each cell group. Means that within the same conditions and not sharing a common superscript symbol(s), differ significantly at *p < 0.05, p < 0.01 vs. control. Superscripts represent significant post-Hoc one-way ANOVA results of improvement over time. Data was analyzed using Duncan's method for post-hoc analysis to compare various groups with each other.

These molecular changes support the activation of both intrinsic and extrinsic apoptotic cascades. Importantly, the exosome-encapsulated form of CINAM exhibited superior potency compared to the free drug, reducing the IC_{50} and enhancing apoptotic indices. This enhancement aligns with recent findings that exosomes improve drug solubility, cellular uptake and intracellular retention [31]. While earlier studies have also shown CINAM-induced G_2/M arrest [32]. Our findings revealed G_0/G_1-phase arrest. This discrepancy may stem from cell line–specific factors or altered cellular internalization dynamics associated with exosomal delivery. Furthermore, EXO-CINAM induced G0/G1 cell cycle arrest, consistent with cinnamaldehyde's role in inhibiting cyclin-dependent kinases and interrupting cell cycle progression [33].

Cinnamaldehyde mostly causes apoptosis by intrinsic routes regulated by the mitochondria, which include activating the caspase-9 and caspase-3 cascades, downregulating anti-apoptotic proteins (BCL-2), and upregulating pro-apoptotic proteins (p53, BAX). In stomach cancer models, it can also cause epigenetic changes and autophagy-mediated cell death [7, 34, 35]. The resulting mitochondrial dysfunction leads to reactive oxygen species (ROS) generation, and subsequent cytochrome c release, activating caspase-9 and downstream caspase-3, hallmark features of mitochondrial-mediated apoptosis [36]. Key molecular factors include mitochondrial malfunction and associated oxidative stress [7, 35]. Moreover, cinnamaldehyde specifically suppresses the PI3K/Akt pathway and modifies cell cycle progression to limit proliferation and promote apoptosis in colorectal cancer [37]. Extrinsic apoptotic signaling is enhanced by upregulating death receptors, such as CD95 (Fas), and their ligands, which complement mitochondrial pathways [38].

At the molecular level, cinnamaldehyde is known to trigger apoptosis through both intrinsic and extrinsic pathways. The extrinsic pathway involves activation of death receptors such as CD95/Fas, leading to caspase-8 activation [38]. The present results showing increased cleaved caspases, p53, BAX upregulation, and BCL-2 downregulation align with these mechanisms and are potentiated by exosome-mediated delivery enhancing CINAM's intracellular availability.

In terms of inflammation and metastasis, our findings showed significant downregulation of NF-κB, MMP-2, MMP-9, and VEGFR2 expression after EXO-CINAM treatment, suggesting reduced tumor invasiveness and angiogenic signaling. These results are consistent with studies indicating that CINAM suppresses NF-κB activation and tumor microenvironment modulation (Cao et al., 2024). The observed reduction in IL-10 levels further supports this immunomodulatory role. However, this contrasts with reports where CINAM elevated IL-10 expression as part of its anti-inflammatory response [39]. Such discrepancies may arise from differences in CINAM dosage, delivery method, or the cancer model employed. Moreover, the marked upregulation of CD95 and CD95L in EXO-CINAM–treated cells reinforce the contribution of the extrinsic apoptotic pathway and complements the findings in other tumor models [40].

The recorded downregulation of NF-κB, MMP-2, MMP-9, and VEGFR2 gene expression after treatment indicates suppression of pro-inflammatory, invasive, and angiogenic signaling pathways, corroborating previous reports of

cinnamaldehyde's multifaceted antitumor effects [41]. The observed reduction in IL-10 also supports a shift in the tumor microenvironment, though this may vary with dose and context [42].

Overall, these data position EXO-CINAM as a promising nanotherapeutic strategy that not only enhances the apoptotic and antiproliferative activity of CINAM but also contributes to the suppression of key molecular pathways involved in inflammation, angiogenesis, and metastasis. This approach may provide a valuable platform for the delivery of hydrophobic phytochemicals in targeted cancer therapy.

The enhanced anticancer efficacy of the exosome-loaded cinnamaldehyde (EXO-CINAM) formulation compared to free CINAM can be explained by several well-established concepts supported by recent literature. Exosomes serve as highly efficient drug delivery vehicles due to their natural origin, biocompatibility, and ability to facilitate targeted cellular uptake and intracellular delivery of therapeutic agents. Haney *et al.,* [22] demonstrated that exosomes improve the solubility and intracellular accumulation of encapsulated compounds, enhancing their bioavailability and therapeutic effects. This delivery advantage likely underlies the increased cytotoxicity and apoptosis induction observed with EXO-CINAM in colorectal cancer cells by promoting more effective drug internalization and retention.

While this study provides valuable insights into the therapeutic efficacy of CINAM-loaded exosomes in colorectal cancer cells, several limitations should be acknowledged. First, all experiments were conducted *in vitro* using a single human colorectal adenocarcinoma cell line (Caco-2). Although this model is well-established for intestinal cancer research, it may not fully represent the complex tumor microenvironment or heterogeneity observed in clinical settings. Second, the pharmacokinetics, biodistribution, and metabolic stability of EXO-CINAM were not evaluated, which limits the conclusions about its behavior *in vivo*. Third, although gene and protein expression analyses suggested the modulation of apoptotic, inflammatory, and angiogenic pathways, the underlying mechanisms were not validated using specific inhibitors or gene knockdown approaches. Finally, the safety, immunogenicity, and long-term stability of exosome-based delivery systems remain unexplored in preclinical animal models. These limitations highlight the need for subsequent vivo studies and mechanistic investigations to confirm the therapeutic potential and safety profile of EXO-CINAM for clinical application.

Exosomes have been shown in previous studies to be efficient natural nanocarriers for phytochemicals, enhancing their pharmacokinetic profiles and therapeutic benefits. Nevertheless, the combination of MSC-derived exosomes and cinnamon aldehyde for colorectal cancer, as well as a comprehensive mechanistic analysis like in your paper, continues to be a unique and significant addition. Moreover, exosomes from edible plants, such as ginger and grapefruit, have been shown to function as biocompatible, non-toxic nanocarriers that enhance drug absorption, target inflammatory and malignant areas of the intestine, and shield therapeutic compounds from deterioration. Exosomes produced from ginger, for instance, demonstrated improved transport and therapeutic efficacy in colitis and cancer models while loading doxorubicin with a high encapsulation efficiency through electrostatic interactions. With lower systemic toxicity, these exosomes efficiently transport siRNA and other nucleic acids while maintaining their bioactivity, enabling targeted medication or gene therapy [43, 44].

Exosomes generated from mesenchymal stem cells (MSCs) have been thoroughly investigated for improved drug delivery because of their capacity to overcome biological barriers, evade the immune system, and exhibit tumor tropism. In cancer models, particularly colorectal cancer, their application for loading hydrophobic natural chemicals such as curcumin, resveratrol, and cinnamon aldehyde analogs, has demonstrated enhanced solubility, intracellular uptake, and therapeutic efficiency. Several techniques have been refined for effective payload loading, including sonication, incubation, and electroporation [45, 46].

Exosome encapsulation of phytochemicals, such as curcumin and resveratrol, has been described in several studies; this method overcomes the problems of low solubility and bioavailability. In vitro and in vivo, exosome administration improves anti-inflammatory properties, induces apoptosis, and suppresses tumor growth pathways. The findings underscore the exosome platform's potential to improve stability, targeted delivery, and controlled release of anticancer agents [47, 48].

Future research should focus on validating these *in vitro* findings *in vivo* tumor models to assess

pharmacokinetics, biodistribution, systemic toxicity, and therapeutic efficacy in a physiological context. Additional studies incorporating mechanistic inhibitors or gene silencing approaches are warranted to dissect the exact molecular pathways modulated by EXO-CINAM. Moreover, exploring targeted or surface-engineered exosomes may further improve tumor selectivity and reduce off-target effects of these exosomes. Ultimately, translation into preclinical and clinical frameworks is essential to realize the full therapeutic potential of exosome-based delivery systems in colorectal and other solid tumors.

CONCLUSION

In conclusion, this study shows that the anticancer activity of cinnamon aldehyde (CINAM) against colorectal cancer (CRC) cells is significantly increased by mesenchymal stem cell–derived exosomes (EXO-CINAM). Exosome administration of CINAM resulted in stronger cytotoxicity, cell cycle arrest, and activation of both mitochondrial and death receptor-mediated apoptotic pathways, which also increased its cellular absorption and bioavailability. Additionally, EXO-CINAM successfully inhibited angiogenic, inflammatory, and metastatic signals. Therefore, these results highlight the therapeutic potential of exosome-based nanocarriers for the targeted delivery of natural hydrophobic chemicals in the treatment of colorectal cancer.

LIMITATIONS

Although the present manuscript assessed EXOs' morphology, their marker-based validation was not done (e.g. tetraspanin immunoblot/flow cytometric analysis), therefore, the future work will include more functional biological objectives e.g. Western blot or flow cytometric analysis of CD9, CD63, CD81 and appropriate negative markers to strengthen vesicle identity and purity. Moreover, as a result, authors will call the preparation "MSC-derived small extracellular vesicles (sEVs)" instead of just "exosomes." Purity and marker evaluations will be part of future research.

ACKNOWLEDGEMENTS

The authors gratefully acknowledge the support of all members of the Materials Science and Nanotechnology Department, Faculty of Postgraduate Studies for Advanced Sciences (PSAS), Beni-Suef University, Egypt, and the Biochemistry Department, Faculty of Science, Beni-Suef University, Egypt.

ETHICS APPROVAL AND CONSENT TO PARTICIPATE

The authors followed the ethics of research, approved, and consented to participate in this study with mentioned approval number for animal handling.

AUTHORS' CONTRIBUTIONS

Dr. Ahmed A. G. El-Shahawy conceived the study and designed the research framework. Dr. El-Shahawy and Salwa Ahmed developed the methodology. Salwa Ahmed Mohammed conducted the experimental work. Data analysis and interpretation were performed by Dr. El-Shahawy and Salwa Ahmed and Asmaa M. Mahmoud. Both authors contributed to manuscript drafting. Dr. El-Shahawy, Salwa Ahmed, and Asmaa M. Mahmoud critically reviewed and revised the manuscript for intellectual content. All authors approved the final version for publication and assume full responsibility for the accuracy, integrity, and scientific validity of the work, ensuring that any concerns are properly addressed.

FUNDING

The authors have no affiliation with any organization with a direct or indirect financial interest in the subject matter discussed in the manuscript. The standing research paper was maintained through individual funding.

CONSENT FOR PUBLICATION

The authors approved this version of the manuscript for publication

AVAILABILITY OF DATA AND MATERIAL

The authors emphasize the availability of data and materials

COMPETING INTERESTS

The authors declared no competing interests

This manuscript has not been submitted to, nor is under review at, another journal or other publishing venue.

REFERENCES

1. Cao, L., S. Wei, Z. Yin, F. Chen, Y. Ba, Q. Weng, et al., Identifying important microbial biomarkers for the diagnosis of colon cancer using a random forest approach. Heliyon, 2024. 10(2). https://doi.org/10.1016/j.heliyon.2024.e24713
2. Jarak, I., A.I. Santos, A.H. Pinto, C. Domingues, I. Silva, R. Melo, et al., Colorectal cancer cell exosome and cytoplasmic

membrane for homotypic delivery of therapeutic molecules. International Journal of Pharmaceutics, 2023. 646: p. 123456. https://doi.org/10.1016/j.ijpharm.2023.123456
3. Wolf, A.M., E.T. Fontham, T.R. Church, C.R. Flowers, C.E. Guerra, S.J. LaMonte, et al., Colorectal cancer screening for average-risk adults: 2018 guideline update from the American Cancer Society. CA: a cancer journal for clinicians, 2018. 68(4): p. 250-281. https://doi.org/10.3322/caac.21457
4. Bhat, S.K. and J.E. East, Colorectal cancer: prevention and early diagnosis. Medicine, 2015. 43(6): p. 295-298. https://doi.org/10.1016/j.mpmed.2015.03.009
5. Islam, M.R., S. Akash, M.M. Rahman, F.T. Nowrin, T. Akter, S. Shohag, et al., Colon cancer and colorectal cancer: Prevention and treatment by potential natural products. Chemico-biological interactions, 2022. 368: p. 110170. https://doi.org/10.1016/j.cbi.2022.110170
6. Sadeghi, S., A. Davoodvandi, M.H. Pourhanifeh, N. Sharifi, R. ArefNezhad, R. Sahebnasagh, et al., Anti-cancer effects of cinnamon: Insights into its apoptosis effects. European journal of medicinal chemistry, 2019. 178: p. 131-140. https://doi.org/10.1016/j.ejmech.2019.05.067
7. Peng, J., X. Song, W. Yu, Y. Pan, Y. Zhang, H. Jian, et al., The role and mechanism of cinnamaldehyde in cancer. Journal of Food and Drug Analysis, 2024. 32(2): p. 140. https://doi.org/10.38212/2224-6614.3502
8. Yueyang, M., H. Yaqin, X. Guolian, Z. Wenjian, J. Yang, L. Chen, et al., Glioma angiogenesis is boosted by ELK3 activating the HIF-1 α/VEGF-A signaling axis. BMC cancer, 2023. 23(1): p. 662. https://doi.org/10.1186/s12885-023-11069-w
9. Petrocelli, G., F. Farabegoli, M.C. Valerii, C. Giovannini, A. Sardo, and E. Spisni, Molecules present in plant essential oils for prevention and treatment of colorectal cancer (CRC). Molecules, 2021. 26(4): p. 885. https://doi.org/10.3390/molecules26040885
10. Shojaeian, A., S. Naeimi Torshizi, M.S. Parsapasand, Z.S. Amjad, A. Khezrian, A. Alibakhshi, et al., Harnessing exosomes in theranostic applications: advancements and insights in gastrointestinal cancer research. Discover Oncology, 2024. 15(1): p. 162. https://doi.org/10.1007/s12672-024-01024-x
11. Liang, Z.-x., H.-s. Liu, F.-w. Wang, L. Xiong, C. Zhou, T. Hu, et al., LncRNA RPPH1 promotes colorectal cancer metastasis by interacting with TUBB3 and by promoting exosomes-mediated macrophage M2 polarization. Cell death & disease, 2019. 10(11): p. 829. https://doi.org/10.1038/s41419-019-2077-0
12. Jafarpour, S., S. Ahmadi, F. Mokarian, M. Sharifi, S. Ghobakhloo, M. Yazdi, et al., MSC-derived exosomes enhance the anticancer activity of drugs in 3D spheroid of breast cancer cells. Journal of Drug Delivery Science and Technology, 2024. 92: p. 105375. https://doi.org/10.1016/j.jddst.2024.105375
13. Huang, D., W. Huang, M. Liu, J. Chen, D. Xiao, Z. Peng, et al., Progress of mesenchymal stem cell-derived exosomes in targeted delivery of antitumor drugs. Cancer Cell International, 2025. 25(1): p. 169. https://doi.org/10.1186/s12935-025-03795-x
14. Zayed, M., E. Elwakeel, P. Ezzat, and B.-H. Jeong, Mesenchymal stem cell-derived exosomes as a potential therapeutic strategy for ferroptosis. Stem Cell Research & Therapy, 2025. 16(1): p. 368. https://doi.org/10.1186/s13287-025-04511-2
15. Sankaranarayanan, J., S.C. Lee, H.K. Kim, J.Y. Kang, S.S. Kuppa, and J.K. Seon, Cinnamaldehyde-treated bone marrow mesenchymal-stem-cell-derived exosomes via aqueous two-phase system attenuate IL-1β-induced inflammation and catabolism via modulation of proinflammatory signaling pathways. International journal of molecular sciences, 2024. 25(13): p. 7263. https://doi.org/10.3390/ijms25137263
16. Jahangiri, B., M. Khalaj-Kondori, E. Asadollahi, L.P. Dizaj, and M. Sadeghizadeh, MSC-Derived exosomes suppress colorectal cancer cell proliferation and metastasis via miR-100/mTOR/miR-143 pathway. International journal of pharmaceutics, 2022. 627: p. 122214. https://doi.org/10.1016/j.ijpharm.2022.122214
17. Dimik, M., P. Abeysinghe, J. Logan, and M. Mitchell, The exosome: a review of current therapeutic roles and capabilities in human reproduction. Drug delivery and translational research, 2023. 13(2): p. 473-502. https://doi.org/10.1007/s13346-022-01225-3
18. Schnur, S., V. Wahl, J.K. Metz, J. Gillmann, F. Hans, K. Rotermund, et al., Inflammatory bowel disease addressed by Caco-2 and monocyte-derived macrophages: An opportunity for an in vitro drug screening assay. In vitro models, 2022. 1(4): p. 365-383. https://doi.org/10.1007/s44164-022-00035-8
19. Haddad, M.J., J. Zuluaga-Arango, H. Mathieu, N. Barbezier, and P.M. Anton, Intestinal epithelial co-culture sensitivity to pro-inflammatory stimuli and polyphenols is medium-independent. International Journal of Molecular Sciences, 2024. 25(13): p. 7360. https://doi.org/10.3390/ijms25137360
20. Zhang, L., G. Jiao, S. Ren, X. Zhang, C. Li, W. Wu, et al., Exosomes from bone marrow mesenchymal stem cells enhance fracture healing through the promotion of osteogenesis and angiogenesis in a rat model of nonunion. Stem cell research & therapy, 2020. 11(1): p. 38. https://doi.org/10.1186/s13287-020-1562-9
21. Théry, C., K.W. Witwer, E. Aikawa, M.J. Alcaraz, J.D. Anderson, R. Andriantsitohaina, et al., Minimal information for studies of extracellular vesicles 2018 (MISEV2018): a position statement of the International Society for Extracellular Vesicles and update of the MISEV2014 guidelines. Journal of extracellular vesicles, 2018. 7(1): p. 1535750.
22. Haney, M.J., N.L. Klyachko, Y. Zhao, R. Gupta, E.G. Plotnikova, Z. He, et al., Exosomes as drug delivery vehicles for Parkinson's disease therapy. Journal of controlled release, 2015. 207: p. 18-30. https://doi.org/10.1016/j.jconrel.2015.03.033
23. Bavafa, A., A. Sepehrinezhad, A. Gorji, F. Forouzanfar, and S. Sahab-Negah, Protocol Optimization for Exosome Production from Umbilical Cord Mesenchymal Stem Cells: A Step Toward Clinical Translation. Basic and Clinical Neuroscience, 2025: p. 0-0.
24. Gorgzadeh, A., A. Nazari, A. Ali Ehsan Ismaeel, D. Safarzadeh, J.A. Hassan, S. Mohammadzadehsaliani, et al., A state-of-the-art review of the recent advances in exosome isolation and detection methods in viral infection. Virology journal, 2024. 21(1): p. 34. https://doi.org/10.1186/s12985-024-02301-5
25. Auquière, M., G.G. Muccioli, and A. des Rieux, Methods and Challenges in Purifying Drug-Loaded Extracellular Vesicles. Journal of Extracellular Vesicles, 2025. 14(6): p.

e70097. https://doi.org/10.1002/jev2.70097
26. Kim, T., J.W. Hong, and L.P. Lee, Efficient methods of isolation and purification of extracellular vesicles. Nano Convergence, 2025. 12(1): p. 45. https://doi.org/10.1186/s40580-025-00509-x
27. Zein, R., I. Alghoraibi, C. Soukkarieh, A. Salman, and A. Alahmad, In-vitro anticancer activity against Caco-2 cell line of colloidal nano silver synthesized using aqueous extract of Eucalyptus Camaldulensis leaves. Heliyon, 2020. 6(8). https://doi.org/10.1016/j.heliyon.2020.e04594
28. Orlando, A., M. Linsalata, and F. Russo, Antiproliferative effects on colon adenocarcinoma cells induced by co-administration of vitamin K1 and Lactobacillus rhamnosus GG. International Journal of Oncology, 2016. 48(6): p. 2629-2638. https://doi.org/10.3892/ijo.2016.3463
29. Karameşe, S.A., The Apoptotic Effects of a Proteasome Inhibitor on Caco-2 Colon Carcinoma Cells. Eurasian Journal of Molecular and Biochemical Sciences. 2(1): p. 19-24.
30. Kim, S., H. Lee, J.W. Lim, and H. Kim, Astaxanthin induces NADPH oxidase activation and receptor-interacting protein kinase 1-mediated necroptosis in gastric cancer AGS cells. Molecular medicine reports, 2021. 24(6): p. 837. https://doi.org/10.3892/mmr.2021.12477
31. Shao, J., J. Zaro, and Y. Shen, Advances in exosome-based drug delivery and tumor targeting: from tissue distribution to intracellular fate. International journal of nanomedicine, 2020: p. 9355-9371. https://doi.org/10.2147/IJN.S281890
32. Wu, F., X. Shi, R. Zhang, Y. Tian, X. Wang, C. Wei, et al., Regulation of proliferation and cell cycle by protein regulator of cytokinesis 1 in oral squamous cell carcinoma. Cell Death & Disease, 2018. 9(5): p. 564. https://doi.org/10.1038/s41419-018-0618-6
33. Aggarwal, S., K. Bhadana, B. Singh, M. Rawat, T. Mohammad, L.A. Al-Keridis, et al., Cinnamomum zeylanicum extract and its bioactive component cinnamaldehyde show anti-tumor effects via inhibition of multiple cellular pathways. Frontiers in Pharmacology, 2022. 13: p. 918479. https://doi.org/10.3389/fphar.2022.918479
34. Kim, T.W., Cinnamaldehyde induces autophagy-mediated cell death through ER stress and epigenetic modification in gastric cancer cells. Acta Pharmacologica Sinica, 2022. 43(3): p. 712-723. https://doi.org/10.1038/s41401-021-00672-x
35. Guo, J., S. Yan, X. Jiang, Z. Su, F. Zhang, J. Xie, et al., Advances in pharmacological effects and mechanism of action of cinnamaldehyde. Frontiers in pharmacology, 2024. 15: p. 1365949. https://doi.org/10.3389/fphar.2024.1365949
36. Banerjee, S. and S. Banerjee, Anticancer potential and molecular mechanisms of cinnamaldehyde and its congeners present in the cinnamon plant. Physiologia, 2023. 3(2): p. 173-207. https://doi.org/10.3390/physiologia3020013
37. Li, J., Y. Teng, S. Liu, Z. Wang, Y. Chen, Y. Zhang, et al., Cinnamaldehyde affects the biological behavior of human colorectal cancer cells and induces apoptosis via inhibition of the PI3K/Akt signaling pathway. Oncology reports, 2016. 35(3): p. 1501-1510. https://doi.org/10.3892/or.2015.4493
38. Zhang, W., W. Lei, F. Shen, M. Wang, L. Li, and J. Chang, Cinnamaldehyde induces apoptosis and enhances anti-colorectal cancer activity via covalent binding to HSPD1. Phytotherapy Research, 2024. 38(10): p. 4957-4966. https://doi.org/10.1002/ptr.7840
39. Yu, M.-l., R.-d. Wei, T. Zhang, J.-m. Wang, Y. Cheng, F.-f. Qin, et al., Electroacupuncture relieves pain and attenuates inflammation progression through inducing IL-10 production in CFA-induced mice. Inflammation, 2020. 43(4): p. 1233-1245. https://doi.org/10.1007/s10753-020-01203-2
40. Zhang, R., Q. Liu, T. Li, Q. Liao, and Y. Zhao, Role of the complement system in the tumor microenvironment. Cancer Cell International, 2019. 19(1): p. 300. https://doi.org/10.1186/s12935-019-1027-3
41. Wang, B., M.-Z. Zhao, L.-Y. Huang, L.-J. Zhang, X.-J. Yu, Y. Liu, et al., Exploring cinnamaldehyde: preparation methods, biological functions, efficient applications, and safety. Food Reviews International, 2025. 41(2): p. 615-642. https://doi.org/10.1080/87559129.2024.2409183
42. Mirlekar, B., Tumor promoting roles of IL-10, TGF-β, IL-4, and IL-35: Its implications in cancer immunotherapy. SAGE open medicine, 2022. 10: p. 20503121211069012. https://doi.org/10.1177/20503121211069012
43. Cai, Y., L. Zhang, Y. Zhang, and R. Lu, Plant-derived exosomes as a drug-delivery approach for the treatment of inflammatory bowel disease and colitis-associated cancer. Pharmaceutics, 2022. 14(4): p. 822. https://doi.org/10.3390/pharmaceutics14040822
44. Sarasati, A., M.H. Syahruddin, A. Nuryanti, I.D. Ana, A. Barlian, C.H. Wijaya, et al., Plant-derived exosome-like nanoparticles for biomedical applications and regenerative therapy. Biomedicines, 2023. 11(4): p. 1053. https://doi.org/10.3390/biomedicines11041053
45. Xu, G., J. Jin, Z. Fu, G. Wang, X. Lei, J. Xu, et al., Extracellular vesicle-based drug overview: research landscape, quality control and nonclinical evaluation strategies. Signal Transduction and Targeted Therapy, 2025. 10(1): p. 255. https://doi.org/10.1038/s41392-025-02312-w
46. Ghosh, S., R. Dhar, G. Gurudas Shivji, D. Dey, A. Devi, S.K. Jha, et al., Clinical impact of exosomes in colorectal cancer metastasis. ACS Applied Bio Materials, 2023. 6(7): p. 2576-2590. https://doi.org/10.1021/acsabm.3c00199
47. Ha, D., N. Yang, and V. Nadithe, Exosomes as therapeutic drug carriers and delivery vehicles across biological membranes: current perspectives and future challenges. Acta Pharmaceutica Sinica B, 2016. 6(4): p. 287-296. https://doi.org/10.1016/j.apsb.2016.02.001
48. Nabih, N.W., M.S. Nafie, A. Babker, H.A. Hassan, and S.A. Fahmy, Recent advances in nano vehicles encapsulating cinnamic acid and its derivatives as promising anticancer agents. RSC advances, 2025. 15(26): p. 20815-20847. https://doi.org/10.1039/D5RA02640G